JACS Au
AN OPEN ACCESS JOURNAL OF THE AMERICAN CHEMICAL SOCIETY

pubs.acs.org/jacsau
Article

Phenylboronic Acid-Functionalized Micelles Dual-Targeting Boronic Acid Transporter and Polysaccharides for siRNA Delivery into Brown Algae

Naoto Yoshinaga,* Takaaki Miyamoto, Mami Goto, Atsuko Tanaka, and Keiji Numata*

Cite This: JACS Au 2024, 4, 1385−1395
Read Online

ACCESS | Metrics & More | Article Recommendations | Supporting Information

ABSTRACT: Brown algae play essential roles ecologically, practically, and evolutionarily because they maintain coastal areas, capture carbon dioxide, and produce valuable chemicals such as therapeutic drugs. To unlock their full potential, understanding the unique molecular biology of brown algae is imperative. Genetic engineering tools that regulate homeostasis in brown algae are essential for determining their biological mechanisms in detail. However, few methodologies have been developed to control gene expression due to the robust structural barriers of brown algae. To address this issue, we designed peptide-based, small interfering RNA (siRNA)-loaded micelles decorated with phenylboronic acid (PBA) ligands. The PBA ligands facilitated the cellular uptake of the micelles into a model brown alga, *Ectocarpus siliculosus* (*E. Siliculosus*), through chemical interaction with polysaccharides in the cell wall and biological recognition by boronic acid transporters on the plasma membrane. The micelles, featuring "kill two birds with one stone" ligands, effectively induced gene silencing related to auxin biosynthesis. As a result, the growth of *E. siliculosus* was temporarily inhibited without persistent genome editing. This study demonstrated the potential for exploring the characteristics of brown algae through a simple yet effective approach and presented a feasible system for delivering siRNA in brown algae.

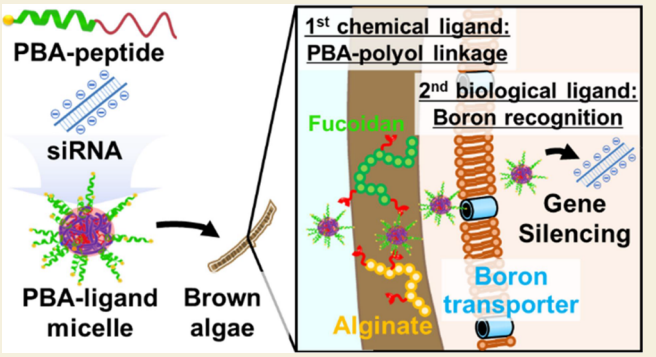

KEYWORDS: *brown algae, siRNA, peptide, phenylboronic acid, micelles, auxin biosynthesis*

Brown algae (phaeophytes) are fascinating organisms that have evolved independently of plants and animals for over one billion years.[1,2] These organisms possess unique morphological structures, sexual systems, and metabolic processes, which can supply valuable resources, such as chemicals for antiviral and antitumor drugs.[3,4] Brown algae also show great potential as a sustainable biofuel resource, offering a viable option for biomass production.[5−7] Furthermore, brown algae significantly helps prevent the release of carbon in the atmosphere through its superior carbon capturing ability; in addition, the turnover of their organic substrates is slow, leading to the entrapment of carbon as "blue carbon" for more extended periods in seawater.[8,9] Brown algae play another important ecological role by providing habitats for other species and serving as primary producers in temperate coastal environments.[10−12] However, the rapid advancement of climate change in recent years has posed a significant threat to brown algae and coastal ecosystems.[13,14] It is therefore crucial to gain more detailed knowledge on the fundamental and physiological characteristics of brown algae to preserve these ecologically and practically invaluable creatures and maximize their utility and tolerability.

One promising approach is to regulate homeostasis in brown algae using genetic engineering tools. However, few effective technologies have been developed, which have seriously impeded fundamental research on brown algae. Very recently, methods employing biolistic bombardment and laser-assisted thermal expansion microinjection have been established to introduce ribonucleoproteins (RNPs) of the clustered regularly interspaced short palindromic repeats (CRISPR)/CRISPR-associated protein 9 (Cas9) system into *Ectocarpus siliculosus* (*E. siliculosus*).[15,16] Researchers have also attempted to deliver small interfering RNA (siRNA) to *E. siliculosus* using a similar approach,[17,18] but no direct evidence of siRNA introduction and gene silencing has been obtained. These techniques suffer from low delivery efficiency, require large equipment, and can be applied only to early developmental cells, such as

Received: December 4, 2023
Revised: February 5, 2024
Accepted: February 20, 2024
Published: March 22, 2024

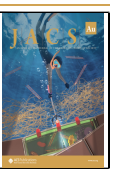

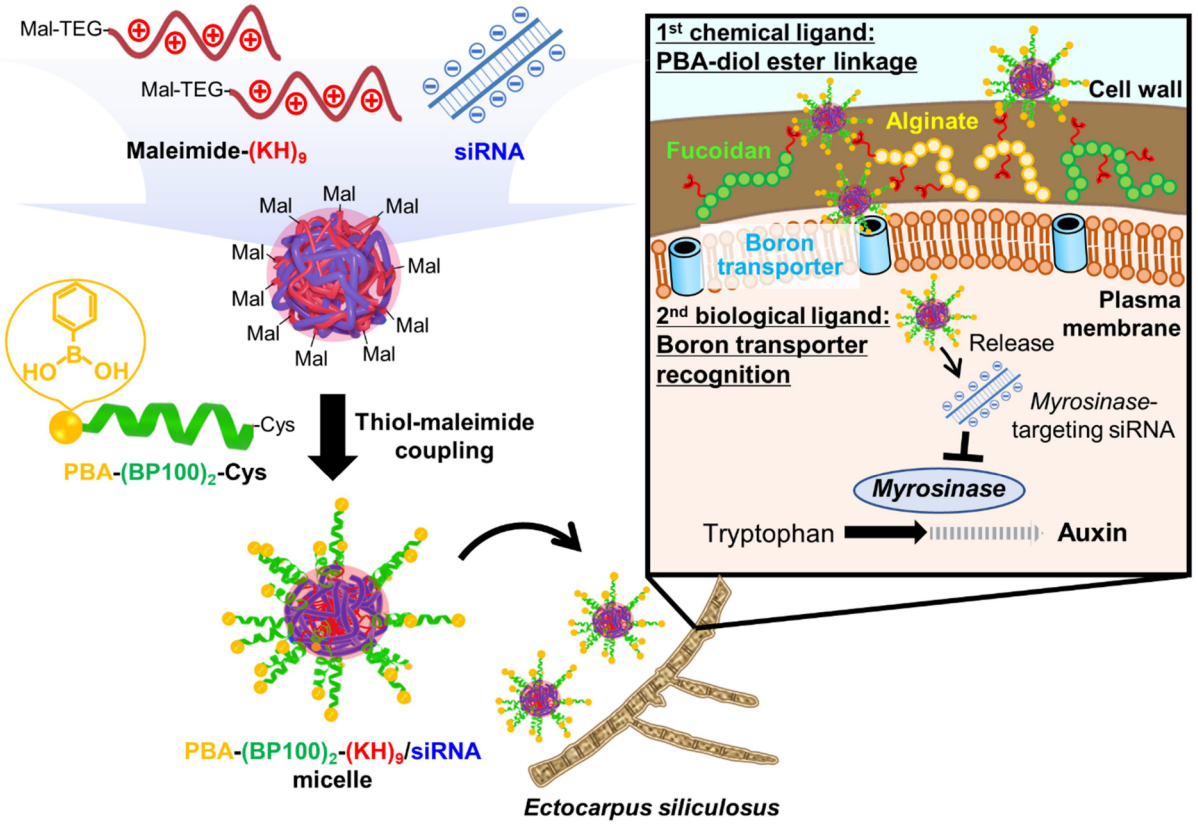

Figure 1. Schematic illustration of the in vivo behavior of siRNA-loaded micelles with PBA ligands in *E. siliculosus*.

gametophytes. Thus, there is a pressing need for advanced systems that can securely deliver biomacromolecules into brown algae.

To address this issue, we developed a novel peptide-based siRNA-loading micelle with a phenylboronic acid (PBA) ligand that targets both polysaccharides in the cell wall, such as fucoidan and alginate,[19−22] and boronic acid transporters on the plasma membrane. PBA is a unique molecule that exhibits pH-dependent shifts between hydrophobic and hydrophilic structures, forming an ester linkage with diol (polyol) compounds in a hydrophilic state.[23−25] Phenylboronate ester formation with polysaccharides in the cell wall may act as a ligand to facilitate the transportation of delivery carriers. Furthermore, brown algae possess boronic acid transporters on the plasma membrane to obtain boronic acid from seawater for nourishment.[26,27] Due to their ability of chemical and biological recognition, PBA moieties make an ideal ligand that can dual-target polysaccharides and boronic acid transporters for solid delivery to brown algae. Here, we decorated the surface of siRNA/cationic peptide complexes with PBA-modified cell-penetrating peptides (CPPs) through maleimide−thiol click chemistry,[28,29] preparing siRNA-loaded micelles. Fusion peptides composed of CPPs and cationic sequence are promising carrier components for the efficient delivery of nucleic acid to organisms with cell walls.[30,31] The PBA moieties were expected to chemically interact with polysaccharides, specifically fucoidan and alginate, to enhance transportation through the cell wall. Boronic acid transporters on the plasma membrane can then recognize the PBA ligands, leading to the smooth uptake of the micelles into the cells (Figure 1). This dual-targeting strategy, especially the ligand effect on boronic acid transporters, dramatically facilitated siRNA uptake into *E. siliculosus* and accomplished effective gene silencing. Consequently, the delivered siRNA targeting an auxin biosynthesis-relevant gene, *Myrosinase*, succeeded in transiently inhibiting the growth of *E. siliculosus* without persistent genome editing. This study is the first to deliver solid siRNA into brown algae, paving the way for siRNA-based genetic engineering to cultivate a better understanding of brown algae.

RESULTS AND DISCUSSION

PBA Modification Fixed Fluorescence Dye into *E. siliculosus*

The ligand effect of boronic acid was first examined by using a fluorescent dye conjugated with PBA. PBA-modified FITC (FITC-PBA) was synthesized according to a previous publication.[27] PBA modification resulted in FITC accumulation in *E. siliculosus*, and accumulation was not achieved with an unmodified dye (Figure 2a). Confocal laser scanning microscopy (CLSM) images indicated that PBA played a dominant role in fixing FITC. To identify the location of FITC-PBA in *E. siliculosus*, we costained the organism with FITC-PBA along with either calcofluor white (CFW) for the cell wall or HCS CellMask for the plasma membrane. CLSM observations showed that the green signal from FITC-PBA overlapped with blue signals from CFW and HCS CellMask (Figures 2b and S1), suggesting that FITC-PBA was located in the cell wall and plasma membrane. Polysaccharides in the cell wall and boronic acid transporters on the plasma membrane are potential candidates that can bind with PBA moieties. To further assess the contribution of PBA, we stained *E. siliculosus* after a 24 h preliminary incubation in seawater with various

https://doi.org/10.1021/jacsau.3c00767
JACS Au 2024, 4, 1385−1395

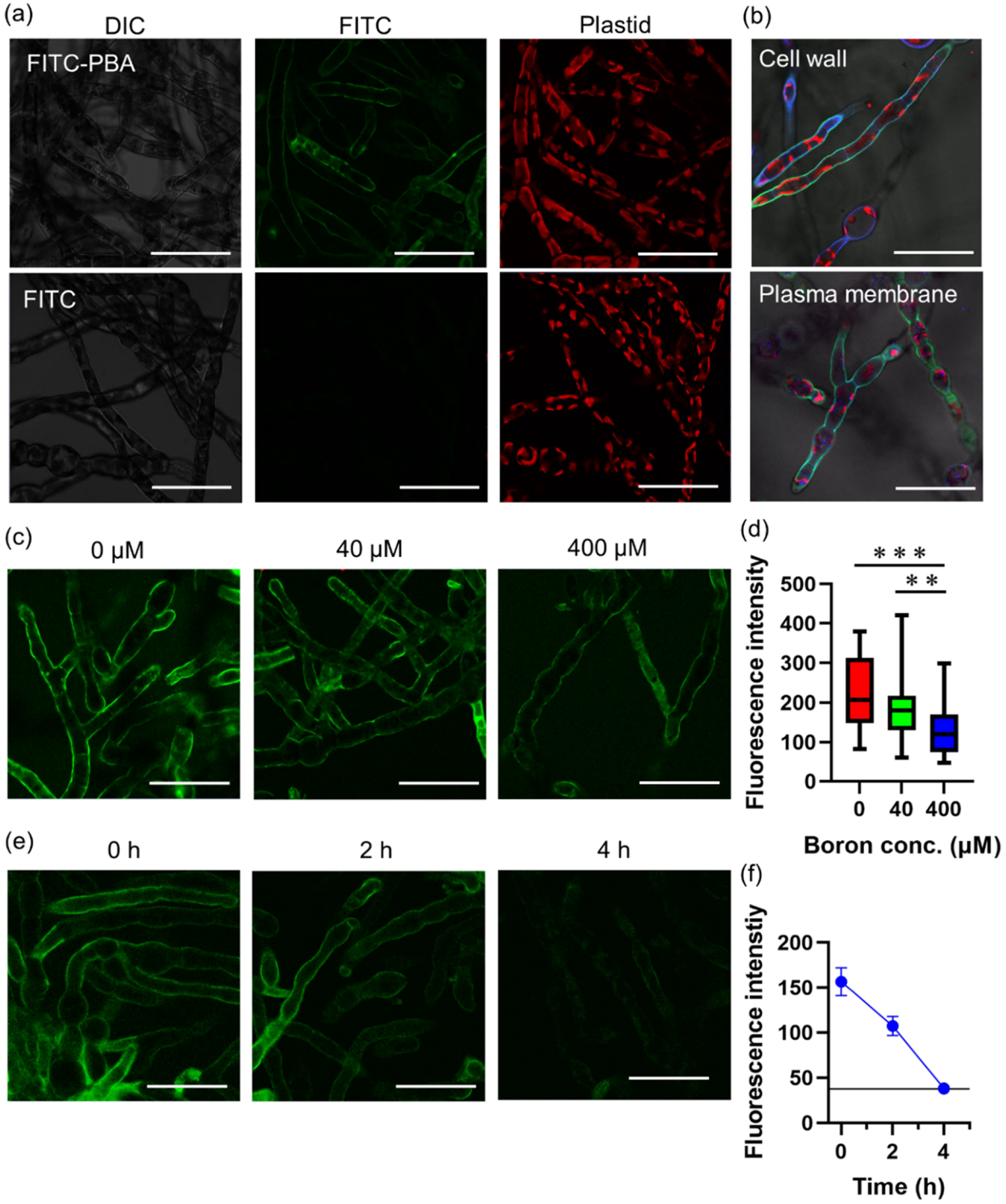

Figure 2. Accumulation of PBA-modified FITC in *E. siliculosus*. (a) CLSM images of *E. siliculosus* after FITC-PBA staining. Green: FITC, red: plastid. (b) Costaining of *E. siliculosus* by FITC-PBA and (top) CFW for the cell wall and (bottom) HCS CellMask for the plasma membrane. Green: FITC-PBA, red: plastid, and blue: CFW or HCS CellMask. (c) CLSM images of *E. siliculosus* stained with FITC-PBA after 24 h of preliminary incubation in seawater with various concentrations of boronic acid (0, 40, and 400 μM). (d) Quantification of the FITC intensity in each *E. siliculosus* sample preliminarily cultured in various concentrations of boronic acid (0, 40, and 400 μM). The FITC intensity was obtained from CLSM images in (c) (n = 40 individual cells). (e) CLSM images of *E. siliculosus* after 2 and 4 h of postincubation from FITC-PBA staining in seawater containing 400 μM boronic acid. (f) Quantification of FITC intensity in each *E. siliculosus* cell 2 and 4 h postincubation from FITC-PBA staining in seawater containing 400 μM boronic acid. The FITC intensity was obtained from CLSM images in (e) (n = 35 individual cells). The solid line in (f) indicates the background value. Scale bars in (a), (b), (c), and (e): 50 μm. Data represent the mean ± SEM $^{**}p < 0.01$ and $^{***}p < 0.001$ (one-way ANOVA with Tukey's post hoc test).

concentrations of nourishing boronic acids (0, 40, and 400 μM). Note that the average boronic acid level in seawater is 430 μM.[32] FITC-PBA accumulation depended on the boronic acid concentration in seawater and was suppressed under high boronic acid conditions (Figure 2c,d). Moreover, we postcultured the FITC-PBA-stained *E. siliculosus* in seawater with 400 μM boronic acid. The green signal from FITC-PBA gradually disappeared within 4 h postincubation (Figure 2e,f),

https://doi.org/10.1021/jacsau.3c00767
JACS Au 2024, 4, 1385−1395

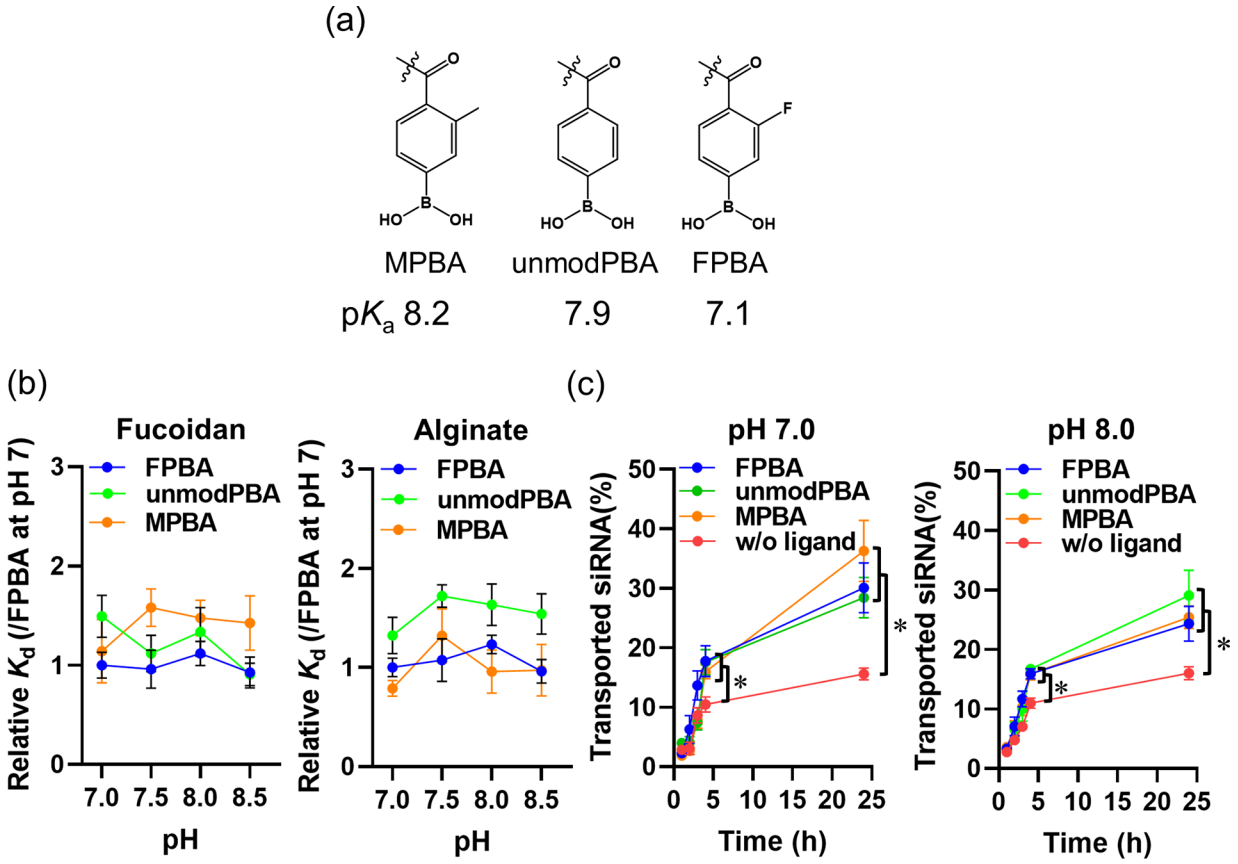

Figure 3. Ligand effect of PBA moieties on polysaccharides in brown algae. (a) PBA derivatives with different pK_a values installed in the N-terminus of CPP. (b) Relative binding coefficient of PBA to fucoidan and alginate at various pH values. Biological replicate (n) = 4. (c) Amount of siRNA transported through the fucoidan/alginate gel at pH 7.0 and 8.0. n = 4. Data represent the mean ± SEM.

Table 1. Characteristics of siRNA-Loaded Micelles[a]

	pK_a of PBA	maleimide conversion (%)	loading capacity (%)	size (d. nm)	PDI	ζ-potential (mV)
$(BP100)_2$-$(KH)_9$		99 ± 1.0	98.0 ± 0.8	41.6 ± 5.2	0.242 ± 0.017	+6.38 ± 2.79
MPBA- $(BP100)_2$-$(KH)_9$	8.2	82 ± 2.6	98.8 ± 0.6	57.7 ± 10.0	0.241 ± 0.019	+7.02 ± 1.71
unmodPBA-$(BP100)_2$-$(KH)_9$	7.9	84 ± 3.0	98.7 ± 0.2	58.1 ± 6.0	0.234 ± 0.041	+6.22 ± 1.51
FPBA-$(BP100)_2$-$(KH)_9$	7.1	81 ± 3.5	98.8 ± 0.4	60.5 ± 8.6	0.239 ± 0.022	+1.39 ± 0.44

[a]Data represent the mean ± SD (n = 4).

indicating that PBA moieties reversibly bound to *E. siliculosus* and competed for nourishing boronic acids in seawater. Through the reversible binding property, PBA-modified molecules could avoid entrapment in the cell wall and on the plasma membrane.

Preparation of siRNA-Loaded Micelles with PBA Ligands

PBA-installed micelles loaded with siRNA were prepared by a two-step procedure according to our previous publication.[28,29] Prior to micelle preparation, a screening test was conducted to determine the uptake efficiency of fusion peptides consisting of various CPPs and nine cationic repeats of a lysine-histidine unit $(KH)_9$. The lysine residues in the cationic segment can electrostatically interact with nucleic acids, and the histidine residues enhance endosomal escape.[29,33] The accumulation of labeled peptides in *E. siliculosus* was observed using CLSM. The screening test showed that $(BP100)_2$-$(KH)_9$ exhibited a higher uptake efficiency into *E. siliculosus* than that of other CPP sequences (Figure S2). $(BP100)_2$ is known to contain β-strand rich structure compared with other tested peptides,[34] which could lead to better cell-penetrating efficiency. The $(BP100)_2$-$(KH)_9$ peptide was used as a platform in the following experiment. A series of PBA ligands with different acid dissociation constants (pK_as) were introduced to the N-terminus of the $(BP100)_2$-cysteine ($(BP100)_2$-Cys) peptide. As phenylboronate ester formation and recognition by boron transporters are sensitive to the structure of boronic acid,[24,35] screening of PBA moieties with different pK_as may provide the optimal formulation for siRNA delivery to brown algae. We chose 4-carboxyPBA (unmodPBA), 4-carboxy-3-fluoroPBA (FPBA), and 4-carboxy-3-methylPBA (MPBA) to conjugate with the N-terminus of $(BP100)_2$-Cys (Figure 3a). The pK_a values of PBA after amide coupling were 7.1, 7.9, and 8.2 for FPBA, unmodPBA, and MPBA, respectively, as determined by the absorbances measured at 268 nm with various pH values (Table 1 and Figure S3).[24] PBA installation to (BP100)2-Cys was confirmed through ^{1}H NMR analysis (2 protons on phenyl ring of PBA: 7.6−7.8 ppm) (Figure S4).

The polyion complex was prepared by mixing siRNA and maleimide-tetra(ethylene glycol)-$(KH)_9$ (Mal-TEG-$(KH)_9$) at a residual charge ratio between cationic amino groups on

https://doi.org/10.1021/jacsau.3c00767
JACS Au 2024, 4, 1385−1395

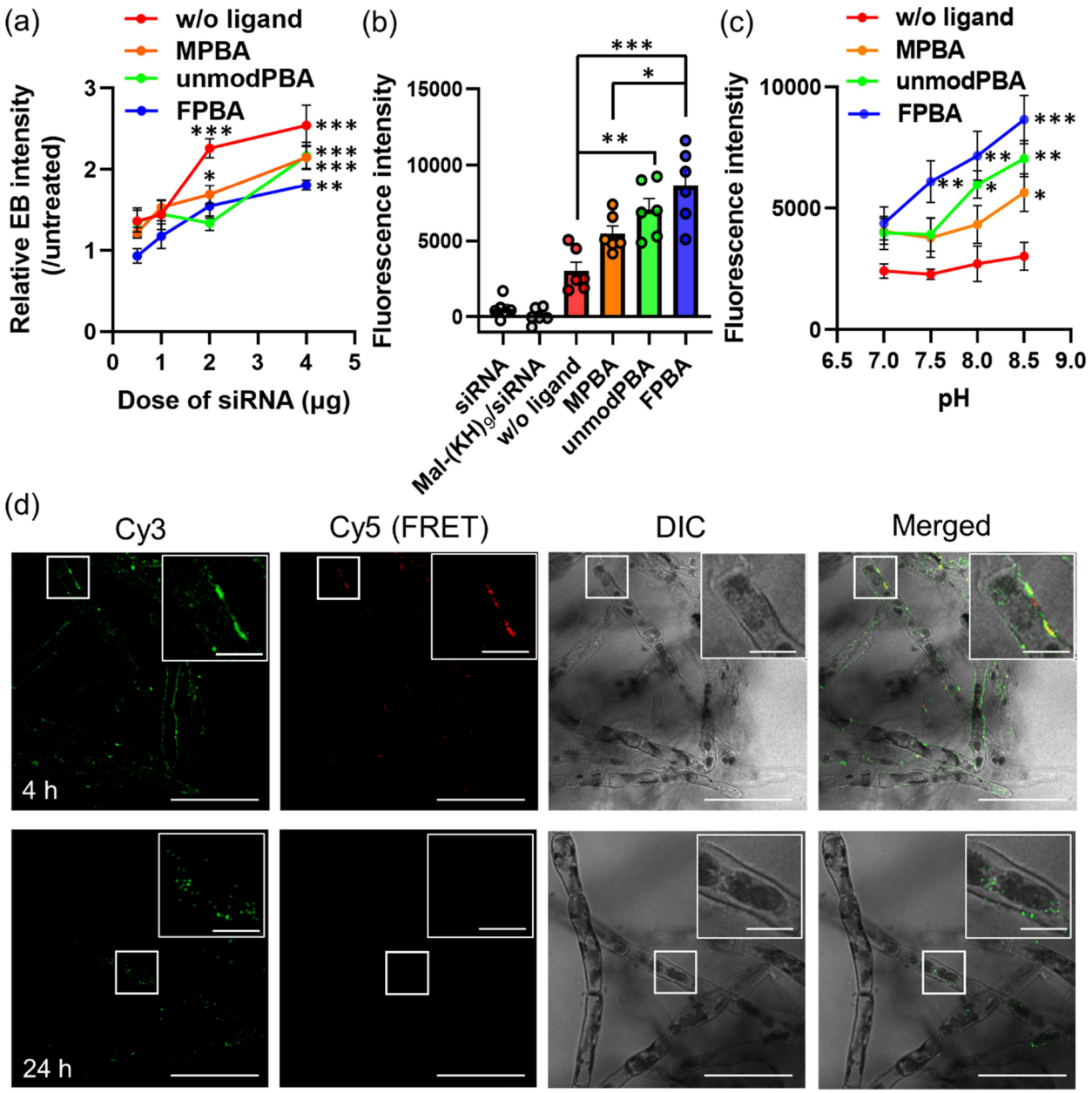

Figure 4. In vivo uptake efficiency of siRNA-loaded micelles by *E. siliculosus*. (a) Toxicity of siRNA-loaded micelles. Biological replicate (n) = 6. (b) Cellular uptake efficiency of Cy5-labeled siRNA. Biological replicate (n) = 6. (c) pH dependency of the cellular uptake efficiency. Biological replicate (n) = 6. (d) Estimation of intracellular siRNA release by observing FRET signals from micelle loading with Cy3- and Cy5-labeled siRNAs excited by 488 nm. Green: Cy3-labeled siRNA and red: Cy5-labeled siRNA (FRET signal). Scale bar: 50 μm in the whole images and 10 μm in the magnified images. Data represent the mean ± SEM *p < 0.05, **p < 0.01, and ***p < 0.001 (one-way ANOVA with Dunnett's post hoc test compared with the untreated group for (a), with the without ligand group for (b), and with each without ligand group under each pH condition for (c)).

peptides and anionic phosphate groups on siRNA (N/P ratio) of 2. Then, 3 equiv. of $(BP100)_2$-Cys with various PBA ligands to the maleimide group was added to the complex solution, and the mixture was shaken for 1 h in 5 mM HEPES buffer (pH 7.8). RP-HPLC charts and MALDI-TOF MS spectra showed that the Mal group was successfully converted, even after complexing with siRNA (Figure S5). The micelle formation was examined by dynamic light scattering measurement. All prepared samples demonstrated a cumulative diameter of 41.6−60.5 nm with a relatively narrow polydispersity index (PDI) (Table 1). Note that 98% or more siRNAs were successfully encapsulated into the micelles. Interestingly, the ζ-potential of the FPBA-modified micelles was lower than that of the other micelles, probably because FPBA, with a lower pK_a value (7.1), had a negatively charged structure at pH 7.8. These results suggested that micelle formation was successful and that PBA ligands were found on the micelle surface.

PBA Ligand Effect on Fucoidan/Alginate for Efficient Transportation

The binding affinity of a series of PBA-modified $(BP100)_2$-Cys to fucoidan and alginate was evaluated by an alizarin red S (ARS) assay.[24] As ARS becomes fluorescent after binding with PBA, the decrease in ARS fluorescence in the presence of

https://doi.org/10.1021/jacsau.3c00767
JACS Au 2024, 4, 1385−1395

competitive diol (polyol) compounds exhibits an exchange reaction between ARS and competitors. The affinity of the diol to PBA can be calculated from the exchange reaction efficiency. Fucoidan and alginate are major components in the cell wall of brown algae and potential candidates that can bind PBA. All PBA-$(BP100)_2$-Cys demonstrated a decrease in ARS fluorescence intensity with increasing fucoidan and alginate levels (Figure S6), which indicated that they were replaced with ARS to form phenylboronate ester linkages. Interestingly, all PBAs showed binding properties similar to those of fucoidan and alginate regardless of pH and pK_a values (Figure 3b). As PBA-diol binding can be strongly affected by ionic strength,[24] the effect derived from various pH and pK_a values was possibly negligible. These results suggested that all designed PBAs could bind to fucoidan and alginate during delivery. Next, we assessed the contribution of the PBA-fucoidan/alginate interaction to the transportation of siRNA-loaded micelles through the cell wall by using Transwell plates. A fucoidan/alginate film was prepared on the upper chamber of Transwell plates,[36] and micelle solutions containing Cy5-labeled siRNA were added. After 4 h of incubation, all PBA-modified micelles exhibited a significantly higher transportation efficiency than those without ligands regardless of pK_a and pH values (Figure 3c), consistent with the PBA binding affinity to fucoidan and alginate. Further incubation for 24 h improved the transportation of the PBA-modified micelles. The chance of contact between the micelles and polysaccharide surface was increased through phenylboronate ester formation, which could enhance access to a fucoidan/alginate layer and lead to higher transportation efficiency. Due to the PBA-polysaccharide interactions, there was a risk that the micelles would fix in the fucoidan/alginate film; however, the risk that the PBA-modified micelles become entrapped may be eliminated by the reversibility of phenylboronate ester. These results indicated that the chemical interaction between PBA-fucoidan/alginate ester formation helped the micelles pass through polysaccharide layers.

Uptake of siRNA-Loaded Micelles into *E. siliculosus*

We investigated the cellular uptake efficiency of siRNA-loaded micelles in *E. siliculosus*. Prior to uptake experiments, micelle toxicity was evaluated through an Evans blue assay.[37,38] *E. siliculosus* was preliminarily cultured in seawater without boronic acid for 24 h before micelle treatment because the interaction between PBA and *E. siliculosus* depended on the boronic acid level in seawater, as shown in Figure 2c,d. The micelles were then transfected in a glucose solution with osmotic pressure similar to seawater to prevent aggregation under high salt conditions. The micelles containing 1 μg or less siRNA did not enhance the internalization of Evans blue into *E. siliculosus*, while those with 2 μg or more siRNA did (Figure 4a). These results indicated that considerable toxicity could occur upon treatment of excess micelles. We used 1 μg or less of siRNA in the following experiments.

We examined the cellular uptake efficiency of the micelles by measuring the fluorescence intensity of the loaded Cy5-labeled siRNA in the total nucleic acid extract. Before the extraction, *E. siliculosus* was treated with RNase A in PBS to completely remove the extracellular siRNA (Figure S7). While no Cy5 intensity was observed in *E. siliculosus* treated with naked siRNA and siRNA/Mal-TEG-$(KH)_9$ complexes, the conjugation of CPP dramatically increased Cy5 intensities (Figure 4b). The introduction of FPBA and unmodPBA ligands, which have lower pK_a values than seawater pH (pH 8.0), further demonstrated the higher uptake efficiency than that of the micelles without ligands. MPBA modification showed some improvement compared with the micelles without ligands, but it was not significant. Competitive boronic acid in the micelle solution prevented cellular uptake (Figure S8), indicating that the PBA ligand helped improve the uptake into *E. siliculosus*.

To gain further insights into the effect of the boronic acid structure on the ligand, the uptake efficiency was assessed under varying pH conditions. While the uptake efficiency of the micelles without ligands was not affected by pH changes, that of PBA-modified micelles depended on pH (Figure 4c). At pH 7.0, all PBA-decorated micelles demonstrated slightly higher uptake efficiency than those without ligands although not significantly. FPBA-modified micelles with a low pK_a value (7.1) showed significantly improved cellular uptake at pH 7.5 or higher. Installing unmodPBA (pK_a: 7.9) resulted in a significantly higher uptake at pH 8.0. The MPBA-modified micelles with a high p*K*a of 8.2 demonstrated enhanced uptake only at pH 8.5 among the tested pH values. These results were consistent with the idea that pH conditions higher than the pK_a value of PBA moieties facilitated the cellular uptake of PBA-modified micelles into *E. siliculosus*.

The uptake efficiency showed a pK_a- and pH-dependent manner although PBA-fucoidan/alginate interactions were independent of the pK_a values (Figure 3b,c). That is, the uptake efficiency was regulated by another factor. The recognition of the PBA ligands by boronic acid transporters probably improved the uptake. A boronic acid transporter identified in *E. siliculosus* recognizes negatively charged boronic acid.[1,26] At seawater pH (pH ∼ 8), 89% of FPBA moieties (pK_a: 7.1) take a negatively charged structure, which may lead to effective recognition by boronic acid transporters. Notably, 56% of unmodPBA (pK_a: 7.9) and 39% of MPBA (pK_a: 8.2) can form a negatively charged structure at seawater pH. Thus, it is reasonable that the biological recognition of PBA moieties by boronic acid transporters was the main factor that improved the cellular uptake efficiency. Note that all PBA-modified micelles, even under pH conditions lower than their pK_a values, showed a minor but not significant enhancement in uptake efficiency. This minor improvement could be attributed to the PBA and fucoidan/alginate interaction because phenylboronate ester formation was independent of the pH and pK_a values (Figure 3). Overall, the results demonstrated that recognition by boronic acid transporters was dominant for the cellular uptake of the micelles, while the chemical binding between PBA and fucoidan and alginate was an ancillary factor.

The intracellular distribution of the PBA-modified micelles was investigated by monitoring FITC-labeled siRNA using CLSM. The green and red pixels correspond to FITC-labeled siRNA and plastids, respectively. Green pixels were observed in the cytosol, demonstrating successful delivery into *E. siliculosus* (Figure S9a). As the acidic compartments in *E. siliculosus*, such as lysosomes, were present as submicron- to micron-sized particles in the cytosol (Figure S9b), most siRNA might escape from acidic compartments except the indicated area by the white arrow in Figure S9a. These results represent the first successful demonstration of the uptake of nucleic acid into brown algae. We further evaluated the siRNA release profile in brown algae by using a Förster resonance energy transfer (FRET) technique. The micelles loading with both Cy3- and Cy5-labeled siRNAs emit significant FRET signals due to the proximal existence of the fluorescence dyes in the core.[39,40]

https://doi.org/10.1021/jacsau.3c00767
JACS Au 2024, 4, 1385−1395

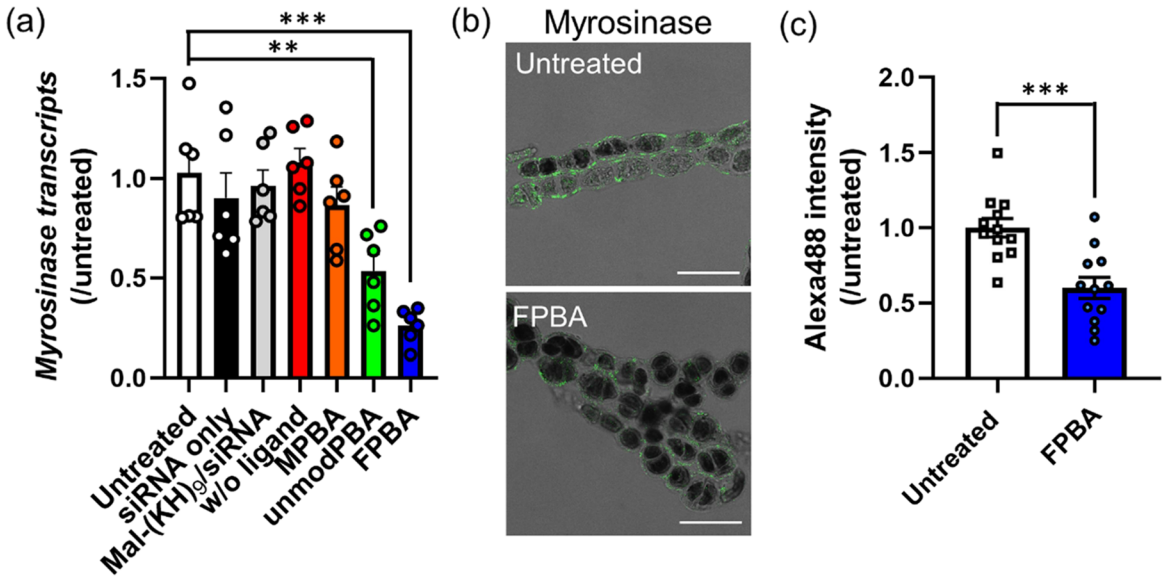

Figure 5. Gene silencing and phenotypic effects on *E. siliculosus*. (a) Quantification of *Myrosinase* transcripts in *E. siliculosus* after 24 h of siRNA treatment. Biological replicate (n) = 6. (b) Representative CLSM images of immunofluorescence staining of Myrosinase (green signal). Scale bar: 50 μm. (c) Immunofluorescence-stained Myrosinase intensity in brown algae. Biological replicates (n) = 12. Data represent the mean ± SEM. Each dot represents biological repeats. ***$p < 0.001$ (unpaired 2-tailed Student's t test).

Encapsulating these siRNAs in the FPBA-modified micelles showed obviously higher FRET efficiency than the mixture of Cy3- and Cy5-labeled siRNAs (Figure S10a). Prior to an *in vivo* observation of the FRET signal, we measured FRET changes in the cell extract. While incubation in a buffer condition and a glucose solution with a similar osmotic pressure to seawater did not affect FRET efficiency, incubation in cell extract dramatically reduced it (Figure S10b). These results raised the expectation of siRNA release from the micelles in brown algal cells. We conducted *in vivo* FRET observation in brown algae using CLSM. The green and red pixels correspond to Cy3-siRNA and Cy5-siRNA excited by 488 nm, respectively. Note that, time gating of plastid autofluorescence allowed precise Cy3 and Cy5 signals.[41] After 4 h of micelle treatment, some green signals overlapped with red ones, which indicated that siRNA still formed a micelle structure (Figure 4d). Meanwhile, other green signals did not colocalize with red ones. As Cy5 fluorescence was observed clearer by excitation at a 633 nm wavelength than 488 nm excitation (Figure S11), both Cy3- and Cy5-labeled siRNAs were successfully delivered in the same cell, and the monitored Cy5 signal by 488 nm excitation was certainly derived from FRET. After 24 h of micelle treatment, although the fluorescence intensity was low, almost no FRET signals were detected, indicating the complete siRNA release in brown algae.

Gene Silencing by *Myrosinase*-Targeting siRNA Treatment

Gene silencing efficiency was examined using siRNA targeting a gene relevant to an auxin biosynthesis pathway. Auxin is an essential plant hormone for the progression of development.[42] The following distinct pathways for auxin synthesis are proposed in terrestrial plants: the YUC pathway, the indole-3-pyruvic acid (IPA) pathway, the indole-3-acetamide (IAM) pathway, and the indole-3-acetaldoxime (TAM) pathway (Figure S12).[43−46] From genome sequence analysis, homologues of genes encoding catalyzing enzymes involved in auxin biosynthesis were inferred in *E. siliculosus*.[42] In this study, we chose a putatively conserved auxin biosynthesis enzyme in the IAOx pathway, *Myrosinase*, as a target gene. The *Myrosinase* sequence was obtained from a previous publication,[1,47] and *Myrosinase*-targeting siRNA with 21 bp was designed by pssRNAit.[48] After 24 h of siRNA-loaded micelle treatment, the amount of *Myrosinase* transcripts was measured by quantitative real-time (qRT)-PCR analysis according to a previous publication.[49] *Myrosinase* transcript reduction was observed only in *E. siliculosus* treated with the unmodPBA- and FPBA-modified micelles (Figure 5a), and FPBA-modified micelles showed a 74% decrease in target gene transcripts. Furthermore, MPBA-modified micelles and those without ligands did not show a decrease in the target transcript. Additionally, naked siRNA and Mal-$(KH)_9$/siRNA complexes exhibited trivial effects. Notably, no gene silencing effect on the target gene was observed for the FPBA-modified micelles loaded with scrambled siRNA (Figure S13a), which indicated that successful gene silencing was achieved through the siRNA delivered by the micelles with PBA ligands.

Gene silencing effect on protein level was evaluated via immunofluorescence staining. Green signals representing immunofluorescence-stained Myrosinase were observed in *E. siliculosus* (Figure 5b). FPBA-modified micelle treatment reduced the fluorescence intensity. Quantification of green signal levels from lysed samples revealed that delivered siRNA decreased approximately half of Myrosinase in protein level (Figure 5c), which was consistent with the gene silencing effect on transcripts (Figure 5a). These results establish a solid outcome in the gene silencing effect by installing PBA ligands.

Phenotypic Effect of *Myrosinase* Gene Silencing on *E. siliculosus* Growth

Auxin, a downstream product of the Myrosinase-relating pathway, was then evaluated using an immunofluorescence technique referring to a previous publication.[42] After 24 h of siRNA treatment, green signals representing immunofluorescence-stained auxin in siRNA-treated *E. siliculosus* seemed weaker than the untreated one (Figure 6a). Quantification of

https://doi.org/10.1021/jacsau.3c00767
JACS Au 2024, 4, 1385−1395

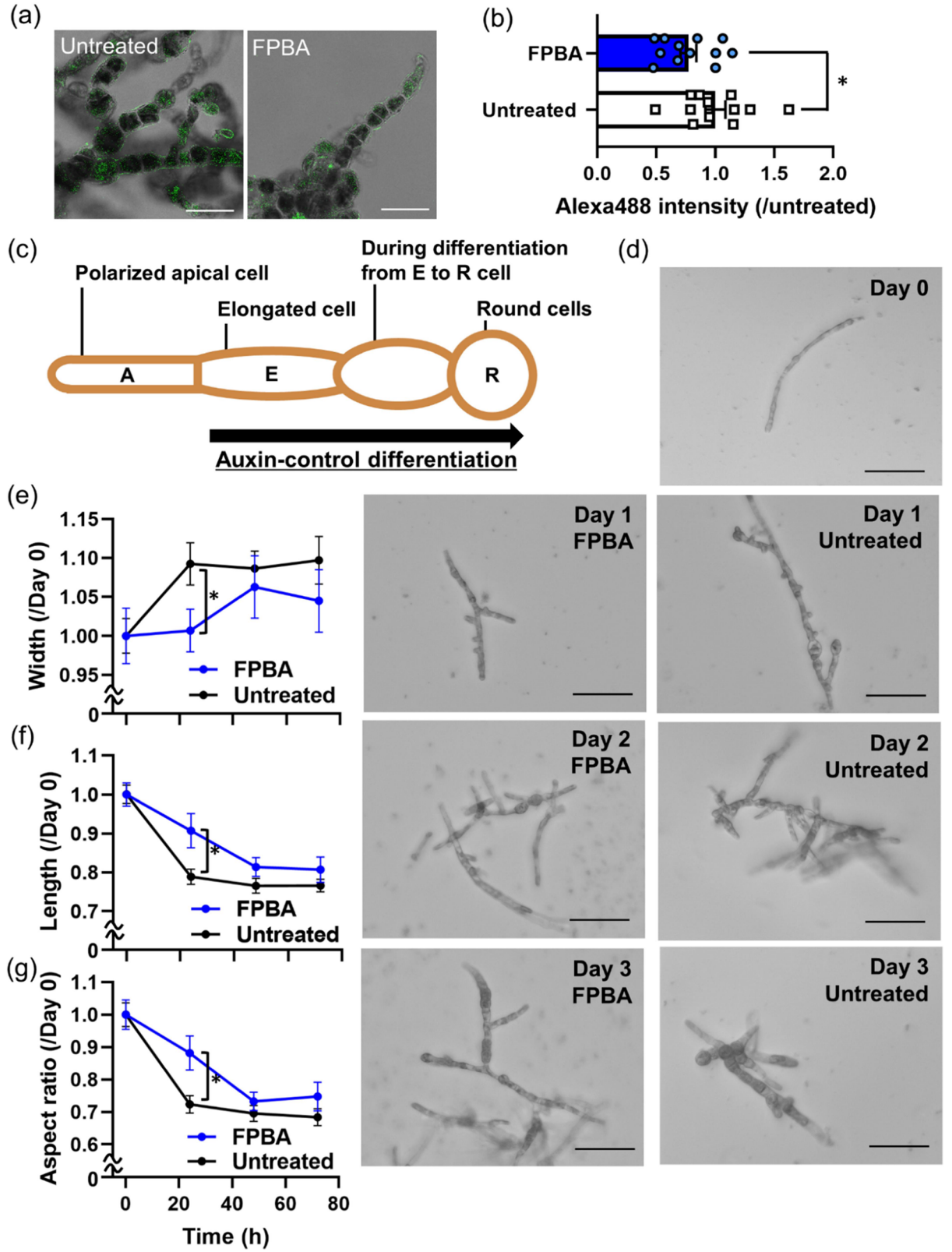

Figure 6. Phenotypic effects on *E. siliculosus*. (a) Representative CLSM images of the immunofluorescence staining of auxin (green signal). Scale bar: 50 μm. (b) Immunofluorescence-stained auxin intensity in brown algae. Biological replicates (n) = 12. (c) Schematic illustration of the effect of auxin on *E. siliculosus* growth. (d) Representative DIC images of *E. siliculosus* after treatment with siRNA-loaded micelles. Scale bar: 100 μm. (e) Width, (f) length, and (g) aspect ratio of *E. siliculosus* obtained from (d). Biological replicate (n) = 10. Data represent the mean ± SEM *p < 0.05 (unpaired 2-tailed Student's t test for (b, e–g)).

the green signal intensity revealed a significant difference between the siRNA-treated sample and the untreated one (Figure 6b). The auxin reduction level by siRNA was limited compared with transcript and protein levels. Other auxin

https://doi.org/10.1021/jacsau.3c00767
JACS Au 2024, 4, 1385–1395

biosynthesis pathways could compensate for IAOx one. The impact of gene silencing on auxin biosynthesis was further evaluated to determine the resulting phenotypic effect. *E. siliculosus* is composed of a prostrate body and an upright body.[42] The prostrate body consists of polarized apical cells, elongated cells localizing at the apexes, and round cells in the center. Auxin regulates elongated cell growth and differentiation to round cells during early development (Figure 5c).[42,50,51] Thus, the length, width, and aspect ratio of each cell should correlate with the auxin biosynthesis efficiency. Following *Myrosinase* gene silencing with FPBA-decorated micelle treatment, the width, length, and aspect ratio were thinner, shorter, and smaller than those of the untreated group (Figure 5d−g). This phenomenon demonstrated that the cells slowly differentiated from elongated to round, demonstrating that inhibition of the IAOx-relevant auxin biosynthetic pathway strongly affected the growth of *E. siliculosus*. Notably, the phenotypic effect did not persist over 48 h (Figure 5d−g). The temporary gene silencing, which was not prolonged over 24 h (Figure S13b), probably allowed for temporary growth control. These results suggested that the IAOx pathway may assume a critical role in *E. siliculosus* growth although the pathway is auxiliary in auxin synthesis in terrestrial plants except for *Brassicaceae*,[46] which raised a clue about auxin biosynthesis in brown algae as well as *E. siliculosus*.

CONCLUSIONS

The significance of brown algae cannot be overstated as the organisms play essential roles in evolution, ecology, and various applications. However, many characteristics of brown algae remain unknown due to the lack of genetic engineering technologies. To address this issue, we developed a PBA-modified micelle loaded with siRNA to regulate the gene expression of a model brown alga, *E. siliculosus*. The PBA ligands chemically and biologically interact with extracellular polysaccharides and boronic acid transporters. The PBA ligand, which achieves multiple and sequential effects, dramatically improves the cellular uptake efficiency of siRNA-loaded micelles. The enhanced siRNA introduction led to efficient gene silencing in *E. Siliculosus* in transcript, protein, and auxin levels, resulting in temporary growth inhibition by *Myrosinase* gene suppression. In this study, nucleic acid was successfully delivered to brown algae with control of homeostasis for the first time.

The developed system is unbound to siRNA delivery. The design principle can potentially be applied to deliver other biomacromolecules such as plasmid DNA, messenger RNA, and proteins. The expansion provides a promising platform and may accelerate progress in the field of brown algae. With the increasing availability of genetic engineering tools, the potential to create advanced strains that produce valuable materials increases. Furthermore, the PBA-ligand strategy established in this study may be adapted to other organisms expressing boronic acid transporters as well as brown algae. The available technology for numerous organisms with boronic acid transporters may provide new opportunities for fundamental and applied research in endlessly interesting algae and plants.

ASSOCIATED CONTENT

Supporting Information

The Supporting Information is available free of charge at https://pubs.acs.org/doi/10.1021/jacsau.3c00767.

Experimental methods,[24,29,49,52−55] co-localization of FITC-PBA with the cell wall and plasma membrane, screening of CPP sequence, pK_a values of PBA, ^{1}H NMR spectra, RP-HPLC charts, MALDI-TOFMS spectra, ARS assay, RNase activity in seawater, effect of boronic acid on cellular uptake of the micelles, CLSM images of micelle cellular uptake, FRET signal of Cy3- and Cy5-labeled siRNA-loading micelles, predicted auxin biosynthesis pathway, gene silencing efficiency at various time points, and peptide sequences used in this study (PDF)

AUTHOR INFORMATION

Corresponding Authors

Keiji Numata − *Biomacromolecule Research Team, RIKEN Center for Sustainable Resource Science, Wako-shi, Saitama 351-0198, Japan; Institute for Advanced Biosciences, Keio University, Tsuruoka-shi, Yamagata 997-0017, Japan; Department of Material Chemistry, Kyoto University, Kyoto-shi, Kyoto 606-8501, Japan;* orcid.org/0000-0003-2199-7420; Email: naoto.yoshinaga@riken.jp

Naoto Yoshinaga − *Biomacromolecule Research Team, RIKEN Center for Sustainable Resource Science, Wako-shi, Saitama 351-0198, Japan; Institute for Advanced Biosciences, Keio University, Tsuruoka-shi, Yamagata 997-0017, Japan;* orcid.org/0000-0003-4399-0289; Email: keiji.numata@riken.jp

Authors

Takaaki Miyamoto − *Biomacromolecule Research Team, RIKEN Center for Sustainable Resource Science, Wako-shi, Saitama 351-0198, Japan;* orcid.org/0000-0002-8192-9342

Mami Goto − *Biomacromolecule Research Team, RIKEN Center for Sustainable Resource Science, Wako-shi, Saitama 351-0198, Japan*

Atsuko Tanaka − *Department of Chemistry, Biology and Marine Science, Faculty of Science, University of the Ryukyus, Nakagami-gun, Okinawa 903-0213, Japan*

Complete contact information is available at: https://pubs.acs.org/10.1021/jacsau.3c00767

Author Contributions

N.Y. and K.N. conceived the project. N.Y., T.M., A.T., and K.N. designed the materials and experiments. N.Y. and M.G. performed the experiments. N.Y. analyzed the data. N.Y. and K.N. wrote the manuscript. All authors have given approval to the final version of the manuscript. CRediT: **Naoto Yoshinaga** data curation, formal analysis, investigation, methodology, writing-original draft, writing-review & editing; **Takaaki Miyamoto** investigation, methodology, writing-review & editing; **Mami Goto** investigation, methodology; **Atsuko Tanaka** methodology, resources, writing-review & editing; **Keiji Numata** conceptualization, funding acquisition, investigation, project administration, supervision, validation, visualization, writing-review & editing.

Notes

The authors declare no competing financial interest.

■ ACKNOWLEDGMENTS

This research was financially supported by the Japan Science and Technology Agency (JST) Exploratory Research for Advanced Technology (JST-ERATO: K.N., Grant Number JPMJER1602), JST COI-Next (K.N., Grant Number JPMJPF2114), The Ministry of Education, Culture, Sports, Science and Technology (MEXT): Data Creation and Utilization-Type Material Research and Development Project Grant Number JPMXP1122714694 (K.N.), JSPS Grant-in-Aid for JSPS Fellowship for Young Scientists (22J00843: N.Y.), and RIKEN Incentive Research Project and Special Post-Doctoral Researcher Fellowship (N.Y.). We appreciate the Support Unit for Bio-Material Analysis, RIKEN Center for Brain Science Research Resources Division, for the peptide synthesis and the use of a Leica TCS SP8 confocal microscope.

■ REFERENCES

(1) Cock, J. M.; Sterck, L.; Rouzé, P.; Scornet, D.; Allen, A. E.; Amoutzias, G.; Anthouard, V.; Artiguenave, F.; Aury, J.-M.; Badger, J. H.; et al. The Ectocarpus genome and the independent evolution of multicellularity in brown algae. *Nature* **2010**, *465* (7298), 617−621.

(2) Bogaert, K. A.; Arun, A.; Coelho, S. M.; De Clerck, O. Brown Algae as a Model for Plant Organogenesis. In *Plant Organogenesis: Methods and Protocols*, De Smet, I., Ed.; Humana Press, 2013; pp. 97−125.

(3) Deniaud-Bouët, E.; Hardouin, K.; Potin, P.; Kloareg, B.; Hervé, C. A review about brown algal cell walls and fucose-containing sulfated polysaccharides: Cell wall context, biomedical properties and key research challenges. *Carbohydr. Polym.* **2017**, *175*, 395−408.

(4) Máximo, P.; Ferreira, L. M.; Branco, P.; Lima, P.; Lourenço, A. Secondary Metabolites and Biological Activity of Invasive Macroalgae of Southern Europe. *Marine Drugs* **2018**, *16* (8), 265.

(5) Song, M.; Duc Pham, H.; Seon, J.; Chul Woo, H. Marine brown algae: A conundrum answer for sustainable biofuels production. *Renewable and Sustainable Energy Reviews* **2015**, *50*, 782−792.

(6) Ji, S.-Q.; Wang, B.; Lu, M.; Li, F.-L. Direct bioconversion of brown algae into ethanol by thermophilic bacterium Defluviitalea phaphyphila. *Biotechnology for Biofuels* **2016**, *9* (1), 81.

(7) Kouhgardi, E.; Zendehboudi, S.; Mohammadzadeh, O.; Lohi, A.; Chatzis, I. Current status and future prospects of biofuel production from brown algae in North America: Progress and challenges. *Renewable and Sustainable Energy Reviews* **2023**, *172*, No. 113012.

(8) Krause-Jensen, D.; Duarte, C. M. Substantial role of macroalgae in marine carbon sequestration. *Nature Geoscience* **2016**, *9* (10), 737−742.

(9) Krause-Jensen, D.; Lavery, P.; Serrano, O.; Marbà, N.; Masque, P.; Duarte, C. M. Sequestration of macroalgal carbon: the elephant in the Blue Carbon room. *Biology Letters* **2018**, *14* (6), No. 20180236.

(10) Harley, C. D. G.; Anderson, K. M.; Demes, K. W.; Jorve, J. P.; Kordas, R. L.; Coyle, T. A.; Graham, M. H. EFFECTS OF CLIMATE CHANGE ON GLOBAL SEAWEED COMMUNITIES. *Journal of Phycology* **2012**, *48* (5), 1064−1078.

(11) He, Q.; Silliman, B. R. Climate Change, Human Impacts, and Coastal Ecosystems in the Anthropocene. *Curr. Biol.* **2019**, *29* (19), R1021−R1035.

(12) Bringloe, T. T.; Starko, S.; Wade, R. M.; Vieira, C.; Kawai, H.; De Clerck, O.; Cock, J. M.; Coelho, S. M.; Destombe, C.; Valero, M.; et al. Phylogeny and Evolution of the Brown Algae. *Critical Reviews in Plant Sciences* **2020**, *39* (4), 281−321.

(13) Froehlich, H. E.; Afflerbach, J. C.; Frazier, M.; Halpern, B. S. Blue Growth Potential to Mitigate Climate Change through Seaweed Offsetting. *Curr. Biol.* **2019**, *29* (18), 3087−3093.

(14) Schlenger, A. J.; Beas-Luna, R.; Ambrose, R. F. Forecasting ocean acidification impacts on kelp forest ecosystems. *PLoS One* **2021**, *16* (4), No. e0236218.

(15) Badis, Y.; Scornet, D.; Harada, M.; Caillard, C.; Godfroy, O.; Raphalen, M.; Gachon, C. M. M.; Coelho, S. M.; Motomura, T.; Nagasato, C.; et al. Targeted CRISPR-Cas9-based gene knockouts in the model brown alga Ectocarpus. *New Phytologist* **2021**, *231* (5), 2077−2091.

(16) Shen, Y.; Motomura, T.; Ichihara, K.; Matsuda, Y.; Yoshimura, K.; Kosugi, C.; Nagasato, C. Application of CRISPR-Cas9 genome editing by microinjection of gametophytes of Saccharina japonica (Laminariales, Phaeophyceae). *Journal of Applied Phycology* **2023**, *35*, 1431−1441.

(17) Godfroy, O.; Uji, T.; Nagasato, C.; Lipinska, A. P.; Scornet, D.; Peters, A. F.; Avia, K.; Colin, S.; Mignerot, L.; Motomura, T.; et al. DISTAG/TBCCd1 Is Required for Basal Cell Fate Determination in Ectocarpus. *Plant Cell* **2017**, *29* (12), 3102−3122.

(18) Macaisne, N.; Liu, F.; Scornet, D.; Peters, A. F.; Lipinska, A.; Perrineau, M.-M.; Henry, A.; Strittmatter, M.; Coelho, S. M.; Cock, J. M. The Ectocarpus IMMEDIATE UPRIGHT gene encodes a member of a novel family of cysteine-rich proteins with an unusual distribution across the eukaryotes. *Development* **2017**, *144* (3), 409−418.

(19) Cumashi, A.; Ushakova, N. A.; Preobrazhenskaya, M. E.; D'Incecco, A.; Piccoli, A.; Totani, L.; Tinari, N.; Morozevich, G. E.; Berman, A. E.; Bilan, M. I.; et al. A comparative study of the anti-inflammatory, anticoagulant, antiangiogenic, and antiadhesive activities of nine different fucoidans from brown seaweeds. *Glycobiology* **2007**, *17* (5), 541−552.

(20) Michel, G.; Tonon, T.; Scornet, D.; Cock, J. M.; Kloareg, B. The cell wall polysaccharide metabolism of the brown alga Ectocarpus siliculosus. Insights into the evolution of extracellular matrix polysaccharides in Eukaryotes. *New Phytologist* **2010**, *188* (1), 82−97.

(21) Chi, S.; Liu, T.; Wang, X.; Wang, R.; Wang, S.; Wang, G.; Shan, G.; Liu, C. Functional genomics analysis reveals the biosynthesis pathways of important cellular components (alginate and fucoidan) of Saccharina. *Current Genetics* **2018**, *64* (1), 259−273.

(22) Lin, Y.; Qi, X.; Liu, H.; Xue, K.; Xu, S.; Tian, Z. The anti-cancer effects of fucoidan: a review of both in vivo and in vitro investigations. *Cancer Cell International* **2020**, *20* (1), 154.

(23) Van Duin, M.; Peters, J. A.; Kieboom, A. P. G.; Van Bekkum, H. Studies on borate esters 1: The ph dependence of the stability of esters of boric acid and borate in aqueous medium as studied by 11B NMR. *Tetrahedron* **1984**, *40* (15), 2901−2911.

(24) Springsteen, G.; Wang, B. A detailed examination of boronic acid−diol complexation. *Tetrahedron* **2002**, *58* (26), 5291−5300.

(25) Yan, J.; Springsteen, G.; Deeter, S.; Wang, B. The relationship among pKa, pH, and binding constants in the interactions between boronic acids and diols—it is not as simple as it appears. *Tetrahedron* **2004**, *60* (49), 11205−11209.

(26) Carrano, C. J.; Schellenberg, S.; Amin, S. A.; Green, D. H.; Küpper, F. C. Boron and Marine Life: A New Look at an Enigmatic Bioelement. *Marine Biotechnology* **2009**, *11* (4), 431−440.

(27) Miller, E. P.; Wu, Y.; Carrano, C. J. Boron uptake, localization, and speciation in marine brown algae. *Metallomics* **2016**, *8* (2), 161−169.

(28) Miyamoto, T.; Tsuchiya, K.; Numata, K. Block Copolymer/Plasmid DNA Micelles Postmodified with Functional Peptides via Thiol−Maleimide Conjugation for Efficient Gene Delivery into Plants. *Biomacromolecules* **2019**, *20* (2), 653−661.

(29) Miyamoto, T.; Tsuchiya, K.; Numata, K. Endosome-escaping micelle complexes dually equipped with cell-penetrating and endosome-disrupting peptides for efficient DNA delivery into intact plants. *Nanoscale* **2021**, *13* (11), 5679−5692.

(30) Numata, K. Poly(amino acid)s/polypeptides as potential functional and structural materials. *Polym. J.* **2015**, *47* (8), 537−545.

(31) Miyamoto, T.; Numata, K. Advancing Biomolecule Delivery in Plants: Harnessing Synthetic Nanocarriers to Overcome Multiscale

https://doi.org/10.1021/jacsau.3c00767
JACS Au 2024, 4, 1385−1395

Barriers for Cutting-edge Plant Bioengineering. *Bull. Chem. Soc. Jpn.* **2023**, *96* (9), 1026−1044.
(32) Argust, P. Distribution of boron in the environment. *Biological Trace Element Research* **1998**, *66* (1), 131−143.
(33) Midoux, P.; Pichon, C.; Yaouanc, J.-J.; Jaffrès, P.-A. Chemical vectors for gene delivery: a current review on polymers, peptides and lipids containing histidine or imidazole as nucleic acids carriers. *Br. J. Pharmacol.* **2009**, *157* (2), 166−178.
(34) Numata, K.; Horii, Y.; Oikawa, K.; Miyagi, Y.; Demura, T.; Ohtani, M. Library screening of cell-penetrating peptide for BY-2 cells, leaves of Arabidopsis, tobacco, tomato, poplar, and rice callus. *Sci. Rep.* **2018**, *8* (1), 10966.
(35) Takano, J.; Miwa, K.; Fujiwara, T. Boron transport mechanisms: collaboration of channels and transporters. *Trends in Plant Science* **2008**, *13* (8), 451−457.
(36) Gomaa, M.; Fawzy, M. A.; Hifney, A. F.; Abdel-Gawad, K. M. Use of the brown seaweed Sargassum latifolium in the design of alginate-fucoidan based films with natural antioxidant properties and kinetic modeling of moisture sorption and polyphenolic release. *Food Hydrocolloids* **2018**, *82*, 64−72.
(37) Lee, H.; Brown, M. T.; Choi, S.; Pandey, L. K.; De Saeger, J.; Shin, K.; Kim, J. K.; Depuydt, S.; Han, T.; Park, J. Reappraisal of the toxicity test method using the green alga Ulva pertusa Kjellman (Chlorophyta). *Journal of Hazardous Materials* **2019**, *369*, 763−769.
(38) Miyamoto, T.; Tsuchiya, K.; Toyooka, K.; Goto, Y.; Tateishi, A.; Numata, K. Relaxation of the Plant Cell Wall Barrier via Zwitterionic Liquid Pretreatment for Micelle-Complex-Mediated DNA Delivery to Specific Plant Organelles. *Angew. Chem., Int. Ed.* **2022**, *61* (32), No. e202204234.
(39) Naito, M.; Yoshinaga, N.; Ishii, T.; Matsumoto, A.; Miyahara, Y.; Miyata, K.; Kataoka, K. Enhanced Intracellular Delivery of siRNA by Controlling ATP-Responsivity of Phenylboronic Acid-Functionalized Polyion Complex Micelles. *Macromol. Biosci.* **2018**, *18* (1), No. 1700357.
(40) Alabi, C. A.; Sahay, G.; Langer, R.; Anderson, D. G. Development of siRNA-probes for studying intracellular trafficking of siRNA nanoparticles. *Integrative Biology* **2013**, *5* (1), 224−230.
(41) Kodama, Y. Time Gating of Chloroplast Autofluorescence Allows Clearer Fluorescence Imaging In Planta. *PLoS One* **2016**, *11* (3), No. e0152484.
(42) Le Bail, A.; Billoud, B.; Kowalczyk, N.; Kowalczyk, M.; Gicquel, M.; Le Panse, S.; Stewart, S.; Scornet, D.; Cock, J. M.; Ljung, K.; et al. Auxin Metabolism and Function in the Multicellular Brown Alga Ectocarpus siliculosus. *Plant Physiology* **2010**, *153* (1), 128−144.
(43) Sugawara, S.; Hishiyama, S.; Jikumaru, Y.; Hanada, A.; Nishimura, T.; Koshiba, T.; Zhao, Y.; Kamiya, Y.; Kasahara, H. Biochemical analyses of indole-3-acetaldoxime-dependent auxin biosynthesis in *Arabidopsis*. *Proc. Natl. Acad. Sci. U. S. A.* **2009**, *106* (13), 5430−5435.
(44) Zhao, Y. Auxin biosynthesis and its role in plant development. *Annu. Rev. Plant Biol.* **2010**, *61*, 49−64.
(45) Mashiguchi, K.; Tanaka, K.; Sakai, T.; Sugawara, S.; Kawaide, H.; Natsume, M.; Hanada, A.; Yaeno, T.; Shirasu, K.; Yao, H.; et al. The main auxin biosynthesis pathway in *Arabidopsis*. *Proc. Natl. Acad. Sci. U. S. A.* **2011**, *108* (45), 18512−18517.
(46) Kasahara, H. Current aspects of auxin biosynthesis in plants. *Biosci., Biotechnol., Biochem.* **2016**, *80* (1), 34−42.
(47) Sterck, L.; Billiau, K.; Abeel, T.; Rouzé, P.; Van de Peer, Y. ORCAE: online resource for community annotation of eukaryotes. *Nat. Methods* **2012**, *9* (11), 1041−1041.
(48) Ahmed, F.; Senthil-Kumar, M.; Dai, X.; Ramu, V. S.; Lee, S.; Mysore, K. S.; Zhao, P. X. pssRNAit: A Web Server for Designing Effective and Specific Plant siRNAs with Genome-Wide Off-Target Assessment. *Plant Physiology* **2020**, *184* (1), 65−81.
(49) Greco, M.; Sáez, C. A.; Brown, M. T.; Bitonti, M. B. A Simple and Effective Method for High Quality Co-Extraction of Genomic DNA and Total RNA from Low Biomass Ectocarpus siliculosus, the Model Brown Alga. *PLoS One* **2014**, *9* (5), No. e96470.
(50) Le Bail, A.; Billoud, B.; Maisonneuve, C.; Peters, A. F.; Mark Cock, J.; Charrier, B. EARLY DEVELOPMENT PATTERN OF THE BROWN ALGA ECTOCARPUS SILICULOSUS (ECTOCARPALES, PHAEOPHYCEAE) SPOROPHYTE1. *Journal of Phycology* **2008**, *44* (5), 1269−1281.
(51) Le Bail, A.; Billoud, B.; Le Panse, S.; Chenivesse, S.; Charrier, B. ETOILE Regulates Developmental Patterning in the Filamentous Brown Alga Ectocarpus siliculosus. *Plant Cell* **2011**, *23* (4), 1666−1678.
(52) Starr, R. C.; Zeikus, J. A. UTEX—THE CULTURE COLLECTION OF ALGAE AT THE UNIVERSITY OF TEXAS AT AUSTIN 1993 LIST OF CULTURES1. *Journal of Phycology* **1993**, *29* (s2), 1−106.
(53) Glüsenkamp, K. H.; Kosegarten, H.; Mengel, K.; Grolig, F.; Esch, A.; Goldbach, H. E. A fluorescein boronic acid conjugate as a marker for borate binding sites in the apoplast of growing roots of Zea mays L. and Helianthus annuus L. In *Boron in Soils and Plants: Proceedings of the International Symposium on Boron in Soils and Plants held at Chiang Mai, Thailand, 7−11 September, 1997*, Bell, R. W.; Rerkasem, B., Eds.; Springer: Netherlands, 1997; pp. 229−235.
(54) Le Bail, A.; Dittami, S. M.; de Franco, P.-O.; Rousvoal, S.; Cock, M. J.; Tonon, T.; Charrier, B. Normalisation genes for expression analyses in the brown alga model Ectocarpus siliculosus. *BMC Molecular Biology* **2008**, *9* (1), 75.
(55) Yoshinaga, N.; Tateishi, A.; Kobayashi, Y.; Kubo, T.; Miyakawa, H.; Satoh, K.; Numata, K. Effect of Oligomers Derived from Biodegradable Polyesters on Eco- and Neurotoxicity. *Biomacromolecules* **2023**, *24* (6), 2721−2729.

https://doi.org/10.1021/jacsau.3c00767
JACS Au 2024, 4, 1385−1395